Journal of
MATERIALS RESEARCH

Atmospheric pressure chemical vapor deposition of TiN from tetrakis(dimethylamido)titanium and ammonia

Joshua N. Musher and Roy G. Gordon
Department of Chemistry, Harvard University, Cambridge, Massachusetts 02138

(Received 15 December 1994; accepted 28 October 1995)

Near stoichiometric titanium nitride (TiN) was deposited from tetrakis(dimethylamido)titanium (TDMAT) and ammonia using atmospheric pressure chemical vapor deposition. Experiments were conducted in a belt furnace; static experiments provided kinetic data and continuous operation uniformly coated 150-mm substrates. Growth rate, stoichiometry, and resistivity are examined as functions of deposition temperature (190–420 °C), ammonia flow relative to TDMAT (0–30), and total gas-flow rate (residence time 0.3–0.6 s). Films were characterized by sheet resistance measurements, Rutherford Backscattering Spectrometry, and X-Ray Photoelectron Spectrometry. Films deposited without ammonia were substoichiometric (N/Ti $<$ 0.6–0.75), contained high levels of carbon (C/Ti = 0.25–0.40) and oxygen (O/Ti = 0.6–0.9), and grew slowly. Small amounts of ammonia (NH_3/TDMAT $\geq$ 1) brought impurity levels down to C/Ti $<$ 0.1 and O/Ti = 0.3–0.5. Ammonia increased the growth rates by a factor of 4–12 at temperatures below 400 °C. Films 500 Å thick had resistivities as low as 1600 $\mu\Omega$-cm when deposited at 280 °C and 1500 $\mu\Omega$-cm when deposited at 370 °C. Scanning electron micrographs indicate a smooth surface and poor step coverage for films deposited with high ammonia concentrations.

I. INTRODUCTION

Nitrides are technologically important materials because of their hardness, stability at high temperatures, chemical inertness, and electrical and optical properties. Transition metal nitrides comprise an important subclass, with applications in wear-resistant, electronic, and optical coatings. Titanium nitride, in particular, is used for tool coating, solar-control films, and microelectronic applications. Optically similar to gold, it is harder than alumina and thermally stable to 3000 °C. TiN is chemically stable with respect to most etching solutions, has a low resistivity, and provides an excellent diffusion barrier against metals. These properties make TiN useful in integrated circuit manufacturing, in which TiN is used as a glue layer for tungsten deposition, and as a diffusion barrier between silicon and metals.

Early chemical vapor deposition (CVD) techniques coated tools by the reaction of $TiCl_4 + N_2 + H_2$ at temperatures above 1000 °C. Many substrates cannot be subjected to such high temperatures. Kurtz and Gordon[1] demonstrated that the deposition temperature could be lowered by introducing preheated ammonia into the gas stream. Reaction (1) allows some less thermally sensitive substrates to be coated, such as glass or unmetallized silicon wafers.

$$6TiCl_4 + 8NH_3 \xrightarrow{500-700^\circ} 6TiN + 24HCl + N_2 \quad (1)$$

Three problems are associated with this process: chlorine contamination, HCl by-products, and high substrate temperatures. Incorporation of chlorine into the film is detrimental to film properties, such as conductivity, and causes delamination from steel substrates. Chlorine corrosion of aluminum over layers is possible. Ammonium chloride by-products form particulates and can cause problems with vacuum pumps and exhaust systems. Lastly, the temperature is still too high for metallized wafers and plastics.

The use of low-temperature physical vapor deposition (PVD) techniques allowed the deposition of TiN on metallized wafers. Reactive sputtering of titanium in a nitrogen atmosphere forms TiN with only a slight dependence on substrate temperature. This process allows for film growth at room temperature.[2] More often, substrate temperatures of 300 °C are used,[3] low enough for metallized silicon wafers.

Deposition methods are severely tested when microelectronic circuit dimensions decrease and aspect ratio (depth/width) of interconnect vias increase. PVD is a line-of-sight process, with sticking coefficients of highly reactive ions close to 1; deposition occurs on the first encountered surface. Material that enters a narrow via will probably hit a wall before reaching the bottom. Voids form as sidewalls thicken and cause failure of devices. A diffusion barrier must coat the entire exposed surface, including hard-to-reach corners. Precise control of incident material directionality can

extend the usefulness of PVD processes. Collimators allow the use of sputtering for 0.35 μm technologies[4] at somewhat reduced growth rates.

PVD barriers fail at lower temperatures than their CVD counterparts because of their columnar structure. A PVD barrier will fail at 350 °C in an Au/TiN/Si metallization scheme,[5] while a CVD barrier can tolerate 550 °C.[6] Raaijmakers and co-workers showed that a PVD barrier needs to be twice as thick as a CVD barrier to provide the same degree of protection.[7]

Despite the higher temperatures required, CVD offers two distinct advantages over PVD for depositing thin films. First, process parameters are less sensitive to fluctuations in CVD. During sputtering, a small shift in nitrogen partial pressure can result in a phase transition in the deposited film.[2,8] Reaction (1) deposits near stoichiometric TiN (N/Ti = 0.95–1.05) under a wide range of conditions.[9] Second, step coverage provided by CVD films is superior to that provided by PVD films.

The $TiCl_4/NH_3$ reaction described earlier is reasonably robust to process irregularities[1] and yields conformal films. A more reactive set of precursors would lower the deposition temperature. Use of methyl-hydrazine in place of ammonia[9] can reduce the reaction temperature by 200 °C, but the chlorine difficulties remain.

An alternative is to replace $TiCl_4$ with a more reactive dialkylamido complex. Bradley and Thomas[10] demonstrated that transamination reactions of various amines with titanium dialkylamides [(2) and (3)] occur in solution, which suggested that the reactions may occur in the

$$\mathrm{M - NR_2 + HNR_2' \longrightarrow M - NR_2' + HNR_2} \quad (2)$$

$$\mathrm{M(NMe_2)_4 + 2RNH_2 \longrightarrow [M(=NR)_2] + 4HNMe_2} \quad (3)$$

gas phase with ammonia. Fix *et al.*[11–13] demonstrated the potential of a low-temperature APCVD process to deposit TiN from tetrakis(dimethylamido)titanium [$Ti(N(CH_3)_2)_4$ or TDMAT] and ammonia. Near-stoichiometric TiN was grown at 1000 Å/min at 200–400 °C, with low levels of oxygen and carbon impurities. In addition to making lower deposition temperatures possible, chlorine and related corrosion problems are avoided.

APCVD, rather than LPCVD, was chosen because of the inherent advantages of an atmospheric pressure system over a low pressure system. Atmospheric pressure processes avoid costly vacuum equipment and allow higher throughputs with a belt furnace. The present study was undertaken to examine the reaction kinetics of the TDMAT + NH_3 system and determine the manufacturing feasibility of the process.

II. EXPERIMENTAL

Films were deposited in a prototype belt furnace from the Watkins-Johnson Company, model WJ-956. The 35-cm wide muffle would accommodate a 30-cm wide substrate without edge effects. An Inconel mesh belt, heated from below, delivered substrates to the deposition zone at 190–480 °C. Reactant gases were injected into the deposition zone approximately 3 mm above the substrate. The injector head was cooled to 110–130 °C, providing a cold-wall reactor configuration. A series of high-volume nitrogen curtains and exhausts prevented laboratory air from reaching the deposition zone.

Precursor gases were injected in an ABA configuration along lines perpendicular to the direction of the motion of the belt (Fig. 1). Diluted ammonia passed through the center line (B) and diluted TDMAT vapor through the outer two lines. In the reverse configuration, only nonconductive orange films could be made. Laminar flow conditions were used (Reynolds number < 30), though some turbulent mixing occurred near the inlets when dilution flows were high. Reactant flows were controlled by mass-flow controllers (Tylan models FC-260 and −261, ±1% stability) and by pressure drops across small diameter tubing (1/8 inch o.d., 0.02 inch i.d., from PhaseSep). Other nitrogen flows were controlled with rotameters from Porter Instruments.

TDMAT (99.999% purity, Schumacher corporation) was placed in a stainless steel bubbler heated with heating tapes controlled by a Watlow 965 time proportional temperature controller. A type K thermocouple placed in a well monitored the bubbler temperature of 80 °C. Precursor vapor pressures were calculated according to Eq. (4).[14] With a temperature stability of ±1 °C, the vapor pressure (3.36 Torr) was kept constant at ±5%. Carrier-gas flow rates were varied to change precursor flow rates; unless otherwise noted, the carrier flow was 1000 standard cubic centimeters per minute (sccm). The carrier gas was diluted with 4.4–14 standard liters per minute (slm) of purified nitrogen after exiting the bubbler. Delivery lines were heated to 100 °C to prevent precursor condensation.

$$\log P_{\mathrm{TDMAT}} = -\left(\frac{2850}{T(\mathrm{K})}\right) + 8.60 \quad (4)$$

Nitrogen was the boil-off from an in-house tank of liquid nitrogen. Purity levels were comparable to purchased UHP nitrogen (<0.5 ppm O_2, H_2O) as measured by a Delta F Trace Oxygen Analyzer (Model FA30111SA) and Meeco Model W Moisture Analyzer. Nitrogen delivered to the deposition zone was purified using Oxiclear and Nanochem purifiers. Long purge times were required to reach the 5 ppb levels claimed achievable by the manufacturers. In practice, impurity concentrations were reduced to the 100 ppb level.

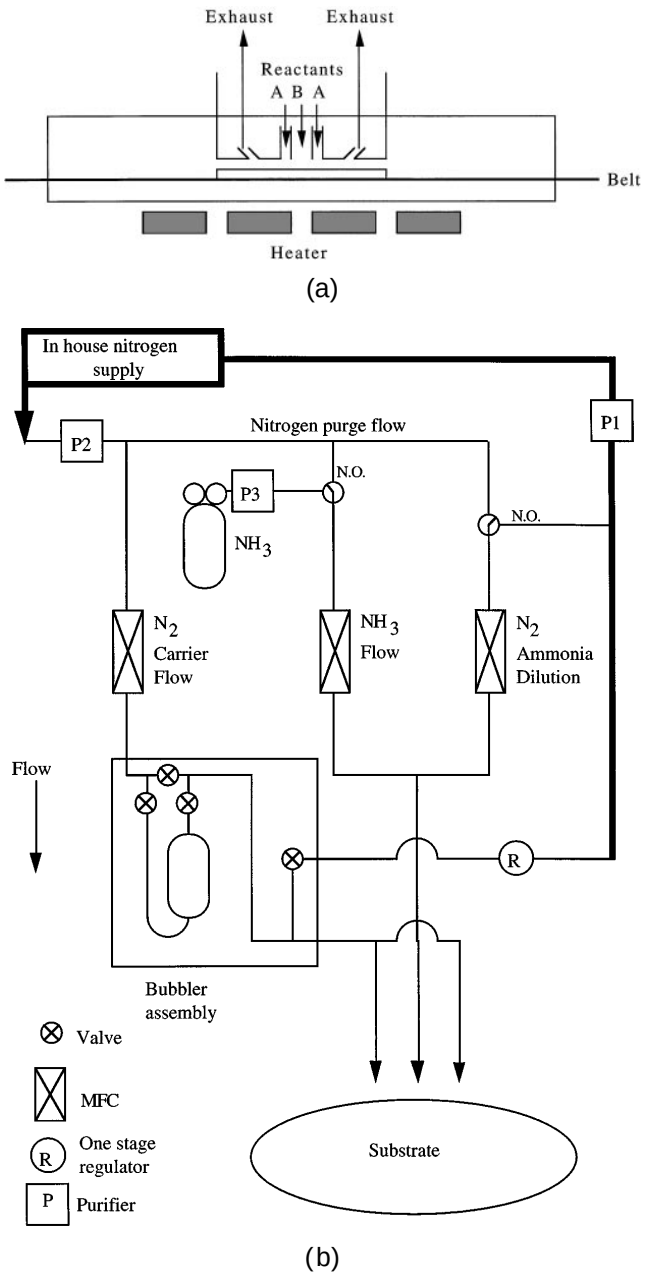

FIG. 1. (a) Schematic of belt furnace. (b) Schematic of gas flow.

Semiconductor grade ammonia (99.995% purity) from Matheson was passed through a Nanochem resin purifier to reduce impurity (specifically oxygen and water) levels to $<$100 ppb. Impurity levels of the ammonia were not measured because of corrosive effects of ammonia on the oxygen meter.

The low tin sides of soda-lime float glass substrates from Kodak (Projector Slide Cover Glass, product number 1402130) were used for sheet resistance, Rutherford Backscattering Spectroscopy (RBS), Forward Recoil Spectroscopy (FRS, or Elastic Recoil Detection), and X-ray Photoelectron Spectroscopy (XPS) measurements. Crystal silicon substrates (p-type, $\langle 100 \rangle$) from Silicon Sense were used for glancing angle and channeling RBS measurements. Wafers for step-coverage measurements from Sematech were returned to Sematech for testing by SEM.

RBS and FRS were conducted in a General Ionix Tandetron Model 4117 at the Cambridge Accelerator for Materials Science in the Materials Research Laboratory at Harvard University. For each spectrum, 4.9 μC of 1.8 and 2 MeV He^+ ions were collected. An Ortec surface barrier detector (FWHM 25–30 keV) placed at 179.5° from the incident beam collected the backscattered ions. The energy spectrum of the reflected particles measured the composition and area density of the deposited film. A Harwell Series I bismuth-implanted standard[15,16] was used to calibrate the titanium area densities. The area density of titanium atoms was converted into a film thickness by $t = N/\rho$, where t is the film thickness, N the area density of titanium atoms determined by RBS, and ρ the density in atoms/cubic centimeter.

RBS cross sections depend on the atomic number of the scattering atom, while the energy of the scattered particle is dependent on the mass of the scattering atom; lighter atoms have smaller cross sections as well as smaller backscattering energies.[17,18] Because hydrogen is lighter than helium, it does not backscatter the incident beam, but recoils forward from the collision. The hydrogen content may be determined by a count of recoiled particles in a forward-scattering geometry (30° from the incident beam).[19] An a-Ge/c-Si sample with 3.7 at.% H (determined by hydrogen evolution) was used to calibrate FRS spectra.

RBS has a low signal-to-noise ratio for nitrogen, oxygen, and carbon on glass and silicon substrates. Sufficiently thin and large boron substrates were not available. XPS measurements, however, can determine the concentrations of these light elements. Surface contamination was removed by sputtering with 3 keV Ar^+ ions for 2 min. Measurements were taken using an SSX-100 ESCA Spectrometer built by Surface Science. Detector width was 12.44 eV with a pass energy of 101.36 eV. The detector was calibrated to the Au $4f^{7/2}$ peak at 84 eV. Data were accumulated for four or eight scans with spot sizes of 600 or 1000 μm.

XPS cross sections are material dependent, so calibration is necessary. RBS at low angles was used to enhance the surface sensitivity of the collected spectrum. Using a scattering angle of 75°, the nitrogen, oxygen, and carbon peaks were easily resolved (Fig. 2). Peak areas indicated a stoichiometry of $TiN_{1.2}O_{0.35}C_{0.05}H_y$ with a relative accuracy of $\pm$10%. The carbon concentration was corrected for an observed increase in peak area during data collection. The stoichiometry from this sample was used to calibrate XPS sensitivities. Sensitivity corrections were 0.84, 0.61, and 0.34 times

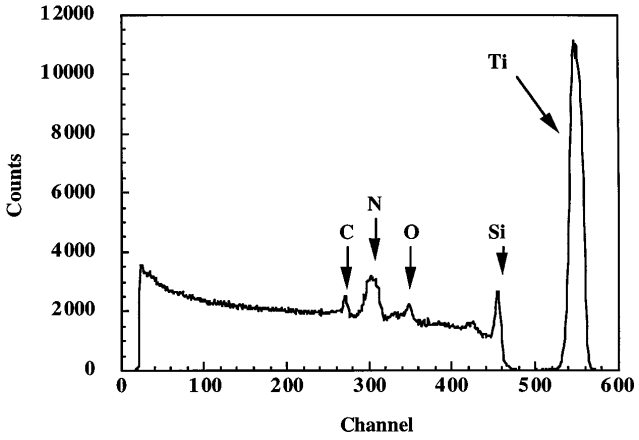

FIG. 2. RBS spectrum taken at glancing angle.

the concentrations determined by Scofield factors for N/Ti, O/Ti, and C/Ti, respectively.

The XPS carbon spectrum could be resolved into several peaks (Fig. 3). The peak at 282.0 eV is associated with titanium carbide (TiC), while peaks at 284–289 eV are from organic carbon (carbon bound to nitrogen, hydrogen, or another carbon). Accumulations of organic carbon (but not carbide carbon) were observed in successive XPS spectra. Usually, four sets of scans were collected, and the carbon areas extrapolated back to zero scans.

Sample thicknesses were determined by low-angle x-ray diffraction (XRD). The modified Bragg condition

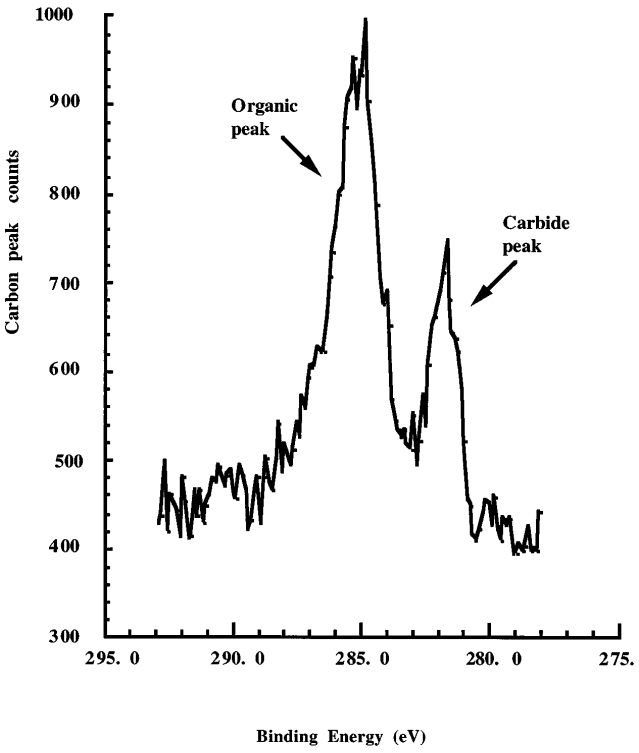

FIG. 3. XPS carbon peak (organic and carbide peaks resolved).

relating the thickness, t, to the nth minima/maxima, θ_n, is

$$\sin^2 \theta_n = \theta_c^2 + (n + \Delta n)^2 \frac{\lambda^2}{4t^2}, \qquad (5)$$

where θ_c is the critical angle for total reflection, and $\Delta n = 1/2$ for a maximum and 0 for a minimum.[20] For films on the order of 100 Å, the diffraction peaks occur at small ($\theta < 5°$) angles. Spectra were collected on a General Electric Diffractometer in a standard θ-2θ configuration using Cr K_α radiation (2.291 Å), and modeled using OM.[21]

Sheet resistance measurements were conducted using a Veeco four-point probe (model FPP-100).

III. RESULTS

Films were deposited for 2 min on 8 cm × 10 cm glass and 15 cm diameter *c*-Si substrates. The resulting films were uniform, within margins of error, in the direction perpendicular to the belt motion. To maximize the understanding of the process and to allow greater flexibility in examining the roles of process parameters, ammonia concentration, temperature, and total gas-flow rate (i.e., time scale for reactions), the belt was held static during the deposition process. Most of the analysis was conducted on these static samples.

Relatively flat thickness and resistance profiles are important because a uniform film is a superposition of films deposited at varying distances from the injection point. Total flow conditions were chosen to meet these criteria while maximizing the deposition rate at specific temperatures. Higher temperatures required larger total flow rates, as shown in Table I. These flow rates spanned the minimum/maximum flows that would yield laterally uniform films in our furnace.

Films appeared brown in transmission when deposited on glass. Films deposited with low ammonia concentrations were more orange in transmitted color. Thicker films deposited with low NH_3 concentrations had a magenta band of reflected color in the middle of the deposition zone, while those deposited with higher ammonia concentrations were golden brown in reflection.

A. Density

Film thicknesses were determined by low-angle x-ray diffraction [Eq. (5)]. Figure 4 shows the spectrum

TABLE I. Gas flow rates and residence times.

Temperature (°C)	Flow rate (slm)	Gas residence time (s)
190	12	0.60
280	16	0.45
370	16–25	0.30–0.45
420	18–25	0.30–0.40

of a 475 Å TiN film on silicon (190 °C, NH_3/TDMAT = 120). The stoichiometry from RBS, $TiN_{1.1}O_{0.3}C_{0.1}H_{0.6}$, was used to calculate density, with a molar mass per titanium atom of 70 amu. The absolute density was calculated according to

$$\text{density} = \frac{\text{area density of Ti atoms}}{\text{thickness}} \times \frac{\frac{\text{amu}}{\text{molecule}}}{N_A\left(\frac{\text{amu}}{\text{gm}}\right)}, \quad (6)$$

where N_A is Avogadro's number (6.02×10^{23}). Using the area density of titanium atoms determined by RBS (0.52×10^{17} atoms/cm^2), the mass density was calculated to be 3.9 gm/cm^3, similar to values obtained by other MOCVD chemistries.[22,23] Knowledge of the density allowed estimation of other film thicknesses using the values for the area density of titanium atoms determined by RBS.

B. Low temperature films

CVD of TiN from TDMAT in the absence of ammonia proceeded slowly at 190 °C. Nitrogen-poor and carbon-containing films were deposited at 25 Å/min. These films were nonconductive, i.e., sheet resistance over 10^5 Ω/square, and had high levels of hydrogen, comparable to the H/Ti ratio (24) in the precursor. These films were too thin to obtain reliable carbon or oxygen contents.

The addition of small amounts of ammonia dramatically increased deposition rates. The growth rate increased by a factor of 12 to 300 Å/min when a 1 : 1 gas volume (1 : 1 molar) NH_3 : TDMAT ratio was used (Fig. 5). Films were still nitrogen-poor (N/Ti = 0.62), but the carbon and carbide (titanium-bound carbon) decreased to less than 10% of the titanium. Resistivities decreased to 5×10^4 μΩ-cm.

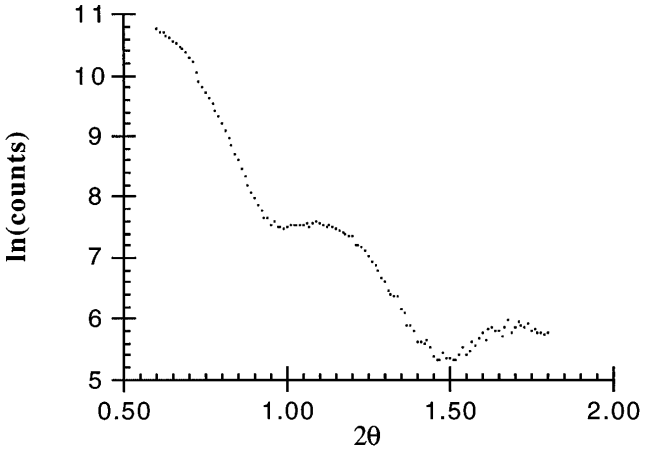

FIG. 4. Low angle x-ray diffraction scan of a film deposited at 370 °C with NH_3/TDEAT = 30.

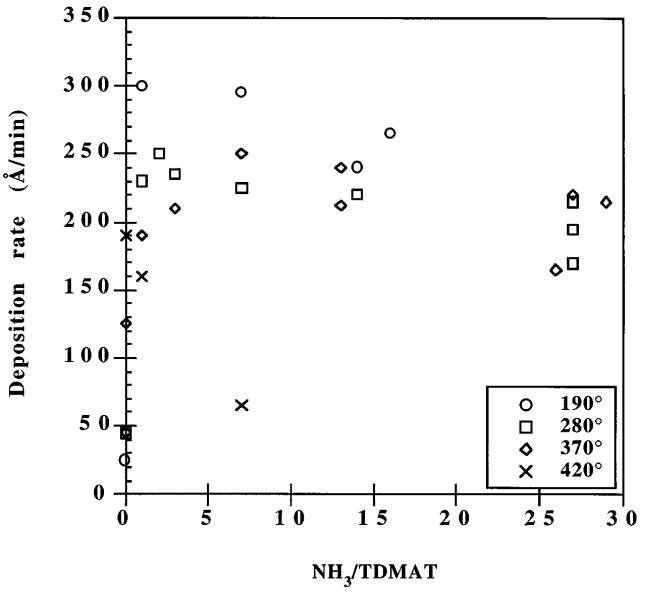

FIG. 5. Film growth rate versus ammonia concentration for different temperatures.

An increase in NH_3 : TDMAT to 7 did not appreciably change the growth rate from the 1 : 1 measurement. Films were still nitrogen poor (N/Ti = 0.89) (Fig. 6), and the carbide concentration increased slightly (Fig. 7); oxygen content (O/Ti) fell by 35% to 0.59 (Fig. 8). Minimum resistivity at the beginning of the deposition region dropped to 5000 μΩ-cm and 2.4×10^4 μΩ-cm at the peak thickness. Higher ammonia concentrations were slightly detrimental to film properties. Growth rates were reduced slightly, and resistivities increased by 20%

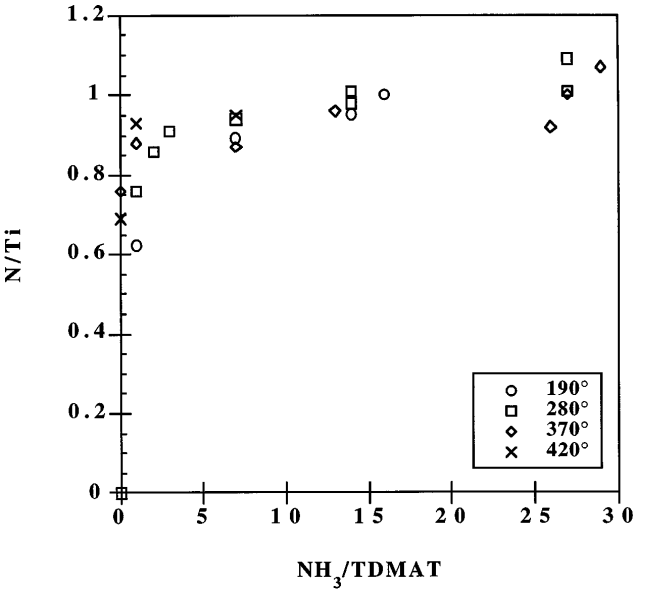

FIG. 6. Nitrogen/titanium ratios versus ammonia concentration for different temperatures.

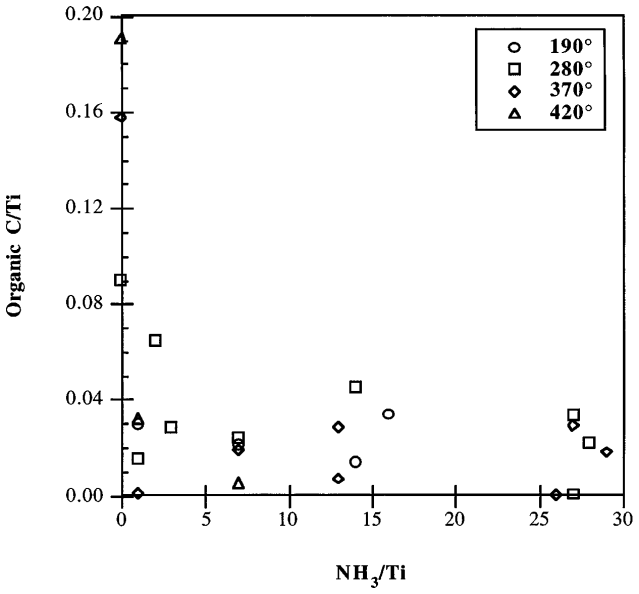

(a)

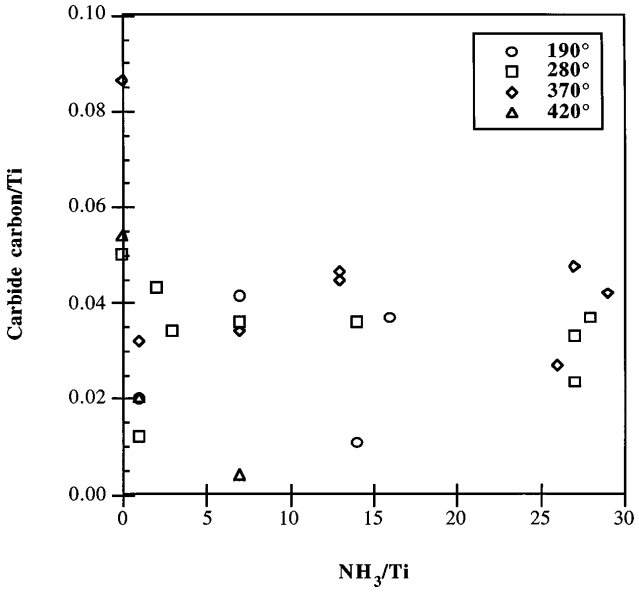

(b)

FIG. 7. (a) Carbon (organic)/titanium ratios versus different NH_3/TDMAT ratios for different temperatures. (b) Carbon (carbide)/titanium ratios versus different NH_3/TDMAT ratios for different temperatures.

when NH_3 : TDMAT reached 14. Hydrogen content decreased sharply with increasing ammonia concentration.

C. Intermediate temperature films

Depositions at 280 °C yielded nitrogen-poor (N/Ti = 0.65) nonconductive films in the absence of ammonia. The growth rate doubled to 50 Å/min from 25 Å/min at 190 °C. A small addition of ammonia (1 : 1 to TDMAT) increased the growth rate (250 Å/min) and

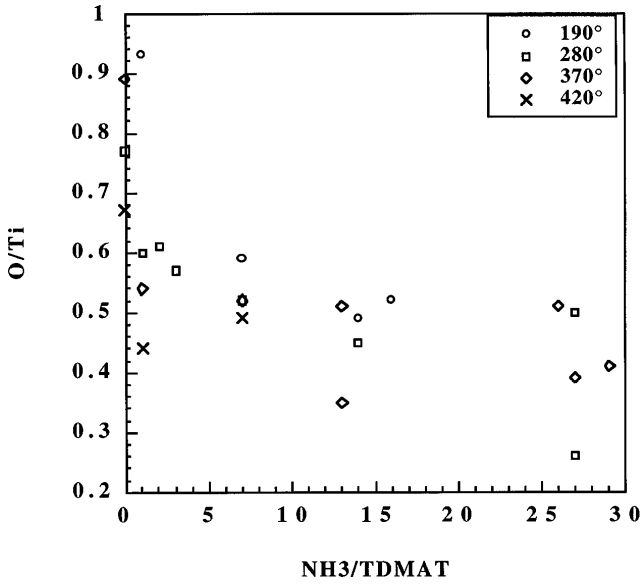

FIG. 8. Oxygen/titanium ratio versus different NH_3/TDMAT ratios for different temperatures.

lowered the resistivity to 3.8×10^4 $\mu\Omega$-cm, similar to what was observed at 190 °C. The stoichiometry improved as the N/Ti increased to 0.76 and the carbon content fell to less than 10% (organic carbon + carbide/Ti). The hydrogen content also decreased.

Further increases in the ammonia concentration did little to increase the growth rate of TiN. Nitrogen concentrations increased (N/Ti = 1.05 ± 0.15) when higher ammonia flows were used (Fig. 6), though no trend was seen in organic or carbide carbon concentrations beyond the significant drop when ammonia was added (Fig. 7). Oxygen content decreased slightly with increasing ammonia (Fig. 8). The hydrogen content, however, dropped by 70% with the increase in ammonia flow (Fig. 9).

Although stoichiometry, except for hydrogen, was not strongly affected by the amount of ammonia present, the resistivity was reduced. Doubling the ammonia concentration ratio from 14 to 28 reduced the resistivity by 40% without an increase in film thickness. Whether higher ammonia flows would reduce the resistivity further is not known.

Film characteristics improved when deposited at 370°. Thin, nonconductive films deposited without ammonia in the reactant stream contained more carbon (organic C/Ti = 0.16, carbide/Ti = 0.09) than films deposited under similar conditions at 280 °C. While still low, the nitrogen concentration (N/Ti = 0.76) was higher than in lower temperature films. A relative ammonia concentration of 1 yielded a near stoichiometric film (N/Ti = 0.88) at the higher deposition rate of 200 Å/min. Carbon contamination was low (C/Ti < 0.05), and oxygen and hydrogen concentrations drop by half in the presence of ammonia.

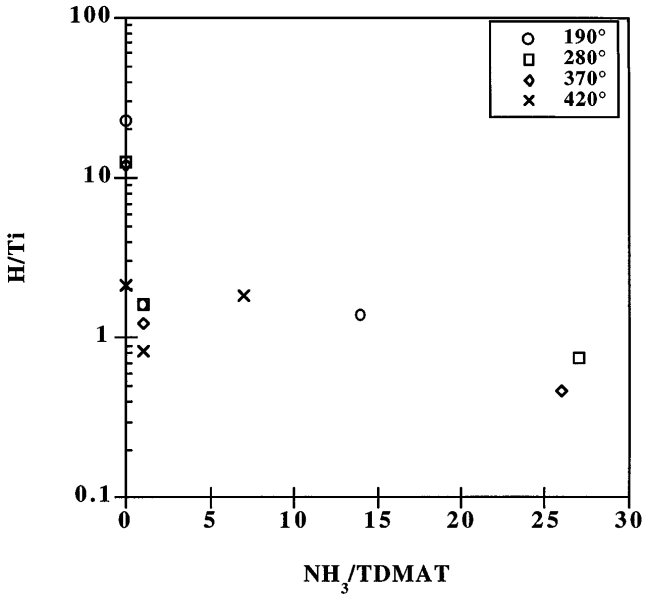

FIG. 9. Hydrogen/titanium ratios versus NH_3/TDMAT ratios for different temperatures.

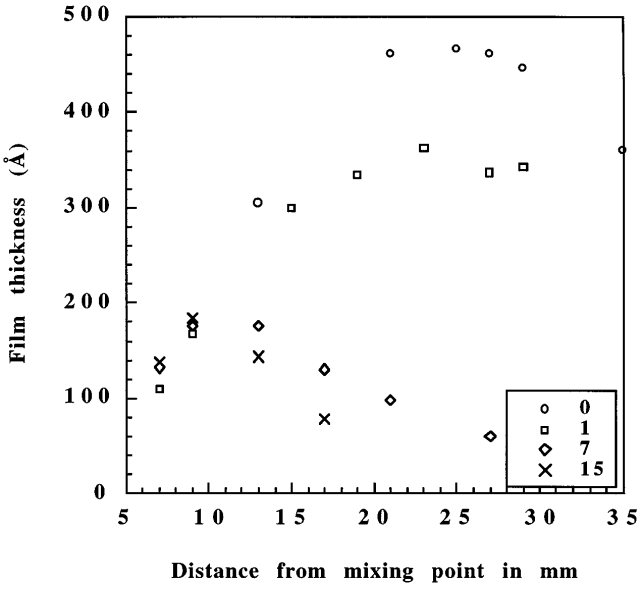

FIG. 10. Film growth profile for different NH_3/TDMAT ratios at 420 °C.

Film resistivity decreased with increases in ammonia concentration. A 90 Å film grown in the absence of ammonia had a sheet resistance above 10^5 Ω/square. Reaction conditions using an ammonia/TDMAT ratio of unity deposited a 380 Å film with a resistivity of 4600 $\mu\Omega$-cm. Film resistivity decreased monotonically with further increases in ammonia concentrations to 1500 $\mu\Omega$-cm at the maximum NH_3/TDMAT = 26 that could be used with our flowmeters.

D. High temperature films

Pyrolytic decomposition of TDMAT became appreciably faster at 420 °C. Conductive films were grown at 150 Å/min without ammonia. Films were nitrogen poor (N/Ti = 0.69), contained carbon (organic C/Ti = 0.19; carbide/Ti = 0.05), and had high oxygen concentrations (O/Ti = 0.62). Film growth started slowly and increased with distance from the injection point (Fig. 10). Despite the relatively high carbon content, the film resistivity was 2900 $\mu\Omega$-cm.

Ammonia reduced the rate of film growth at 420 °C, in contrast to the increased rates observed at lower temperatures. Although the ammonia reduced the impurity concentrations (H, O, C) in the film and increased the nitrogen content (N/Ti = 1.0), it also sped up the reaction. The reaction proceeded too quickly, deposited a film only on the first third of the substrate, and produced more powder, so that the yield of film was reduced. An increase in total (dilution) gas-flow rate did not help to spread out the reaction; a film deposited immediately after the point of mixing, even when the ammonia concentration ratio was unity. Though the film growth rate increased slightly, the resistivity increased to 3750 $\mu\Omega$-cm.

Additional ammonia continued these trends. Film stoichiometry improved with decreasing concentrations as the carbon and carbide, but resistivity increased to 5700 $\mu\Omega$-cm with an ammonia concentration of 0.13%. Film growth occurred primarily within the first 0.3 s after gas mixing at only 65 Å/min, so that the actual amount of titanium deposited in the reaction zone decreased by a factor of 4.

E. Stability

Sheet resistances were measured within a few minutes after deposition. Subsequently, an increase in resistance was observed in many, but not all, the films. Resistances for very thin films could increase within minutes. Thicker films generally increased in resistance over the course of hours or not at all. The increases in resistance were completed within 12–24 h from the initial measurement. Films deposited with large ammonia concentrations and higher temperatures were more stable with time (Fig. 11).

IV. DISCUSSION

A. Growth rates

APCVD film growth is significantly slower than traditional PVD methods. Reactive sputtering can deposit films at 10,000 Å/min,[24] whereas CVD growth rates are only 2% of this. High growth rates, however, yield poor step coverage. Sputtering systems must be collimated to deposit conformal films in high-aspect-ratio struc-

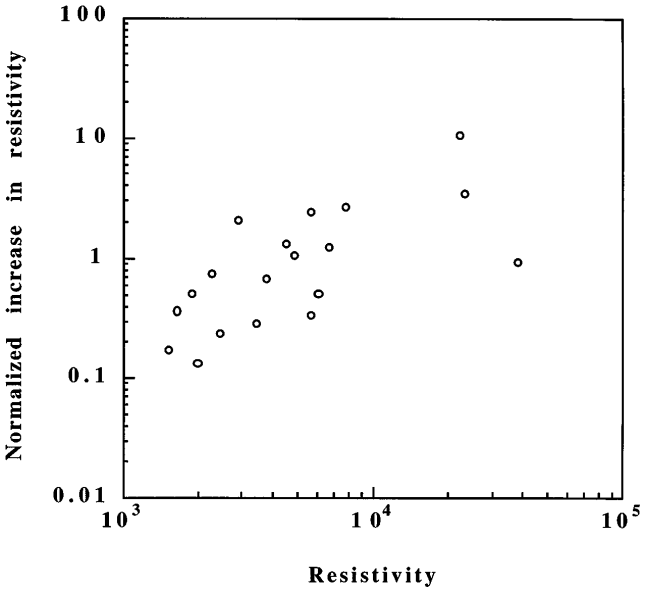

(a)

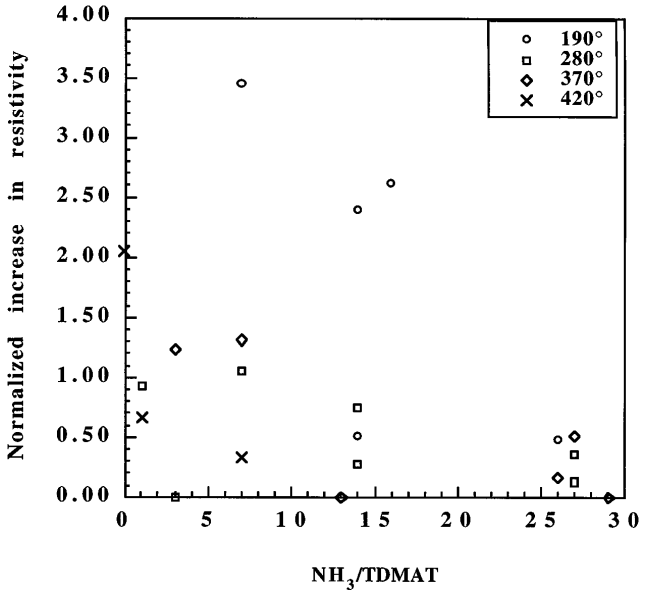

(b)

FIG. 11. (a) Normalized increase of resistivities $[(\rho_f - \rho_i)/\rho_i]$ versus initial resistivity. (b) Normalized increase of resistivities $[(\rho_f - \rho_i)/\rho_i]$ versus NH_3/TDMAT ratio.

tures. A collimator, however, reduces the growth rate to 200 Å/min,[24] eliminating the advantage sputtering holds in deposition rates over CVD processes. The collimator needed for 0.25 μm geometries will undoubtedly lead to even fewer titanium atoms reaching the substrate surface, making the growth rates comparable to CVD films. Other deposition processes have lower growth rates, e.g., pulsed laser ablation of TiN targets deposits films at 60 Å/min.[25]

LPCVD processes can deposit films at 1000 Å/min,[26] although lower rates (100 Å/min) generally lead to higher quality films.[27] The high deposition rates by CVD are often achieved by using a high precursor flow rate (20–30 sccm) and a low residence time. By comparison, we grew 250–300 Å/min films using only 4.2–4.7 sccm of TDMAT vapor.

Film-growth rates from pure TDMAT depend on temperature. Growth increased from 25 Å/min at 190 °C to 150 Å/min at 420 Å (Fig. 5) under similar flow conditions. Under flow conditions optimized for flat resistance profiles at high ammonia concentration, ammonia increased film-growth rates by a factor of 12 at 190° to a factor of 4 at 370 °C. The growth rate increased slightly (20%) at 420 °C, and the deposition pattern shifted to the beginning of the deposition zone; little deposition occurred at the end of the substrate.

The presence of small ammonia concentrations was sufficient to increase the growth rate, although the actual concentration was secondary. Above a critical level, higher ammonia flows decrease the film thickness (the number of deposited titanium atoms). The trend was slight but apparent. The variation was not due to a change in density, because RBS measures the number of atoms per square centimeter, and an otherwise determined (assumed constant) density yields a thickness. Changes in density would affect the thickness: the increase in density generally associated with high ammonia-reactant concentrations would mean a thinner actual film was deposited.

Another measure of film growth is the deposition efficiency, defined as the number of atoms deposited on the substrate surface divided by the incident flux of precursor atoms. The total number of titanium atoms deposited on the surface was calculated using the area densities found by RBS. Typically, five points were taken at 10, 16, 20, 24, and 30 mm from the center. The endpoints of deposition were taken to be 7 and 38 mm. Integration was performed using the trapezoidal rule.

The total amount of film deposited closely follows the trends described above for peak growth rates. Conversion of titanium atoms in the gas phase to titanium atoms on the substrate was ~10% for a wide range of process parameters. The highest efficiencies were observed with ammonia/TDMAT ratios between 7 and 14. Approximately one out of six incident titanium reactant atoms were deposited on the substrates when 33 sccm of ammonia were diluted with 20 slm of nitrogen at 370 °C. Conversion rates in the absence of ammonia increased with temperature from 1% at 190° to 12% at 420°.

B. Stoichiometry

TiN films deposited without ammonia were nitrogen-poor and contained oxygen, carbon, and hydrogen. In-

creased temperatures yielded higher N/Ti ratios, but the films remained substoichiometric.

Ammonia in the reactant stream is crucial to the deposition of stoichiometric TiN. Films deposited with ammonia were close to stoichiometric TiN. The nitrogen content increased with ammonia concentration. This effect saturated quickly (NH_3/TDMAT $\leqslant$ 14) when N/Ti $= 1.0 \pm 0.1$, consistent with most CVD studies, which use large (>10) excesses of ammonia to yield overstoichiometric TiN.[11–13,23,26,27] Relative ammonia concentrations above 14 show a slight upward trend in N/Ti (Fig. 6).

High oxygen concentrations were found in films deposited without ammonia. A small amount of ammonia reduced the oxygen content by 20–40%. Further increases in the ammonia concentration produced a slight trend similar in magnitude but opposite in direction to that of N/Ti (Fig. 8).

The oxygen content is an important issue. Generally associated with increasing film resistivities, oxygen also plays a key role in the barrier properties of TiN.[6,8,28] Oxygen was incorporated into the sample during growth, and also after deposition for those films that were porous (see Sec. IV. D). Gaseous oxygen concentrations in the exhaust from the deposition zone were below 2 ppm. Improved balancing of the nitrogen curtain flows, longer purge times, and a slower belt speed all would help reduce the oxygen present during film growth.

A minimum gas-phase ratio of 1 : 1 NH_3/TDMAT was sufficient to change the reaction process and almost eliminate carbon contaminants. Carbon and carbide contents dropped to less than 10% of the titanium concentrations when ammonia was added to the reactant stream. Katz and co-workers[26] reported a reduction in carbon with an NH_3/TDMAT of 1.5%. Above a ratio of 1 the effect appears saturated, with no trend detectable above the noise. The transamination reactions in solution seen by Bradley and Thomas[10] evidently occur readily in the gas phase as well.

One effect of temperature was to reduce the amount of ammonia needed before reaching stoichiometric TiN. The relative ammonia-concentration threshold is about 7 for the higher temperatures, and 14 at 190 °C (Fig. 6).

Hydrogen was the only constituent with a dependence on both ammonia concentration and temperature (Fig. 9). An increase in either produced a decrease in the residual hydrogen in the film by 15–75%. The nitrogen and oxygen contents showed slight trends, respectively, increasing and decreasing with higher ammonia concentrations (Figs. 6 and 8). No trend was seen in the carbon data (Fig. 7).

C. Resistivity

Resistivity, unlike stoichiometry and film growth, was appreciably dependent on the deposition temperature and the amount, not just the presence, of ammonia (Fig. 12). Films deposited without ammonia had high resistivities. Below 420 °C, the introduction of ammonia reduced resistivities by an order of magnitude or more. The effect began to saturate at 0.5% NH_3 (NH_3/TDMAT = 14), although the exact point was a function of temperature. An increase in deposition temperature resulted in a decrease in resistivity to a minimum (1500 $\mu\Omega$-cm) at 370 °C. A further increase in temperature raised resistivity.

Resistivity was moderate (2900 $\mu\Omega$-cm) when TiN was deposited from TDMAT alone at 420 °C. In contrast to the effect at lower temperatures, ammonia increased resistivity by a factor of 2.

Our minimum resistivity (1500 $\mu\Omega$-cm) compared poorly with PVD films, which can be grown with resistivities as low as 40–100 $\mu\Omega$-cm in room-temperature processes.[29] One explanation is the high degree of stoichiometric control in PVD systems. CVD films are often only near stoichiometric (N/Ti $= 1.1 \pm 0.15$) and can contain impurities (Cl, C, O, and H).[9,11–13,23,26,27] Figure 13 shows a high correlation between stoichiometry (N/Ti) and resistivity. Hydrogen contents are often 25–100% of the titanium concentrations,[12,27] and may affect the electrical parameters of the film (Fig. 14).

D. Artifacts in the data

Some caveats for interpreting stoichiometry and film resistivity must be mentioned. The relative elemental concentrations determined by XPS are subject to two sources of error: scattering cross sections are sensitive to the chemical environment, and a standard similar to the material in question is necessary to determine accurate

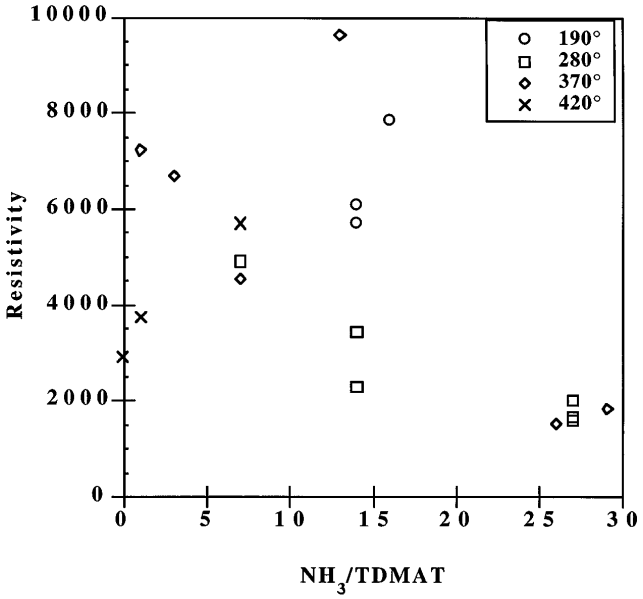

FIG. 12. Minimum resistivities versus ammonia concentration.

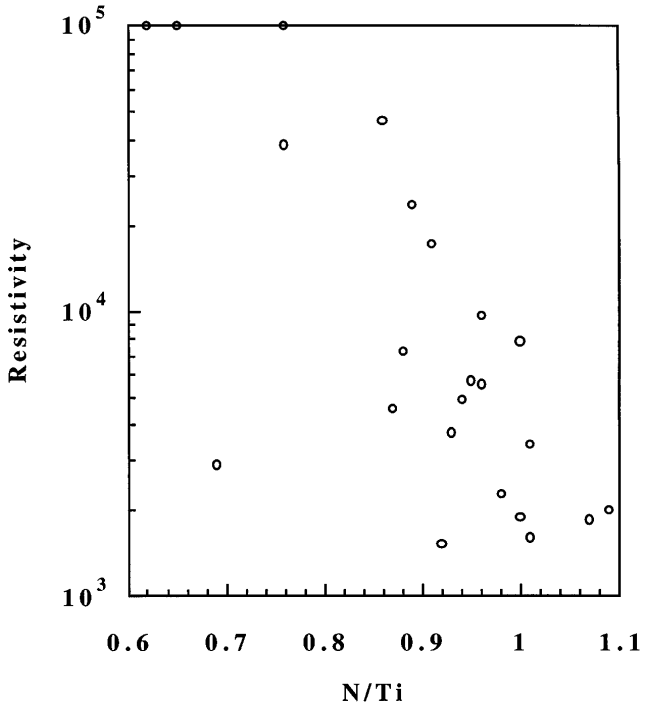

FIG. 13. Resistivity ($\mu\Omega$-cm) versus N/Ti.

atomic proportions. In addition, preferential sputtering of light atoms may occur, which would explain the slightly higher titanium concentrations seen in XPS. A depth profile showed little change in atomic composition after 2 min of sputtering (Fig. 15), suggesting that little preferential sputtering occurred. The slight decrease in carbon concentrations may be due to a reduction in carbon accumulation rate while in the XPS chamber, which in turn is due to an overall decrease in chamber pressure. The RBS calibration should remain valid if

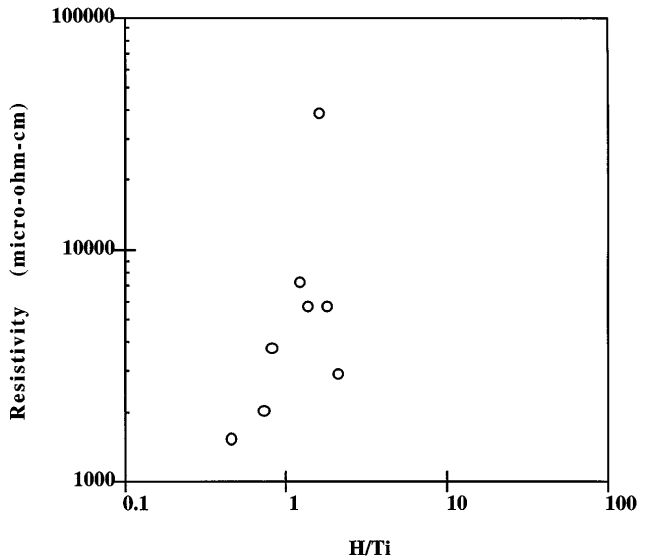

FIG. 14. Resistivity ($\mu\Omega$-cm) versus H/Ti.

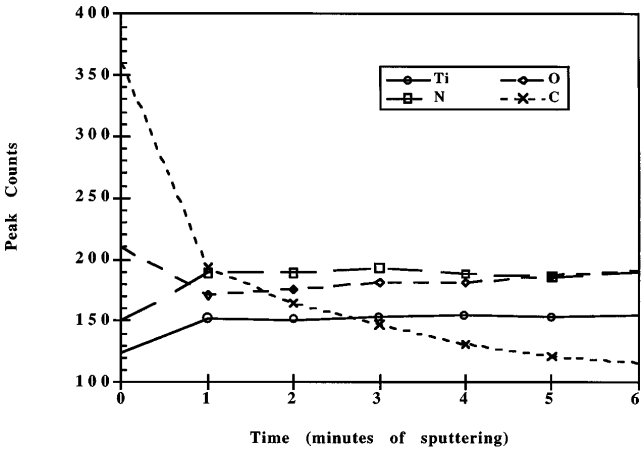

FIG. 15. Depth profile showing change in atomic composition with depth.

the scattering cross sections and preferential sputtering remain insensitive to chemical composition.

The oxygen content and the resistivity may be affected by growth conditions and properties of a specific sample and should be generalized to other films with caution.

The growth rate is an important parameter in thin-film processing. Strongly dependent on temperature and reactant concentrations, the growth rate affects the incorporation of impurities. This effect is called impurity segregation when growing a crystal from a melt. In CVD, the incorporation of contaminants (e.g., oxygen) may be related to the growth rate with either a positive or a negative correlation.

Carrier and reactant gases include $\sim$100–500 ppb of water and oxygen as they enter the reaction zone. Incorporation of these contaminants into the film was controlled by the same processes that governed film deposition. The reaction of titanium with oxygen and water are fast enough that titanium is often used as a gettering material to remove these impurities. The upper bound to the ratio of oxygen atoms (from molecular oxygen and water) to titanium atoms in the gaseous reaction zone during deposition was less than 10%, while the O/Ti ratio for high growth rate conditions was about 1/3. Thus the oxygen to titanium ratio in the films is higher than the gas phase. This result may be due, at least in part, to oxygen having a higher sticking probability than titanium during film growth.

Although high growth rates generally lead to higher concentrations of impurities in crystal growth from the melt, the reverse is often true in CVD. High film growth rates supply more of the desired components, reducing the percentage of impurities incorporated into the film from the carrier gas. Low film growth rates allow the same supply of contaminants, resulting in higher concentrations in the film. Films deposited without ammonia

grew under the latter set of conditions and incorporated larger volumes of oxygen.

Another source of oxygen in the films is exposure to air after the deposition has been completed. Sheet resistance was measured within 5 min after the substrate exited the furnace. Measurements were repeated after at least 12 h. Many films showed an increase in sheet resistance, presumably due to oxidation. The effect could be dramatic; resistance increased by the minute on one film deposited without ammonia. Thin films were especially vulnerable to surface oxidation. Sputtering removed the surface oxide layer for XPS analysis, but was not effective for porous films made in the absence of ammonia, which oxidized throughout the thickness of the film.

Although the resistances were measured within 5 min after the sample exited the furnace, the samples were exposed to the atmosphere after exiting the primary muffle and before exiting the secondary (cooling) muffle. Because the exposure occurs at elevated temperatures (50–100 °C), some film oxidation may occur before the substrate exits the furnace.

E. Mechanism

The thermal decomposition of TDMAT may involve the β-hydride elimination reaction (7).

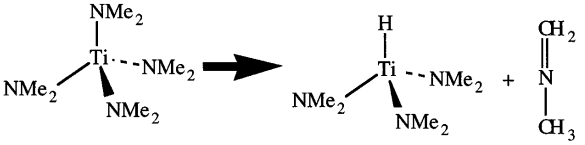

(7)

The insertion reaction in reaction (8) is supported by infrared spectroscopy studies of TDMAT thermal decomposition in the gas phase.

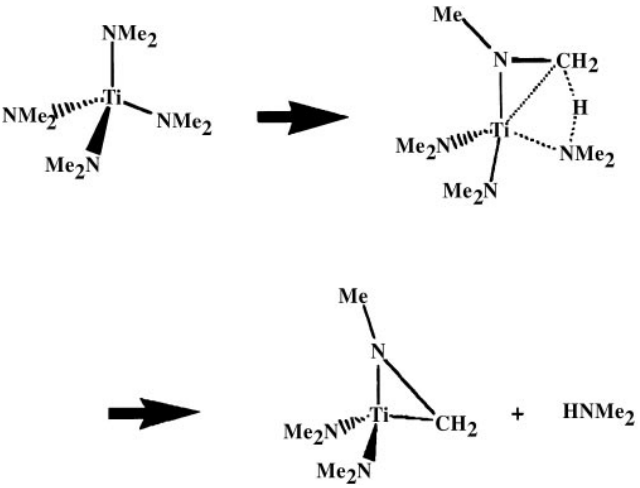

(8)

A band at 1276 cm^{-1} was assigned to Ti–N–C rings by analogy to the thermolysis of the related tantalum compound $Ta(NMe_2)_5$.[30] The strong Ti–C bond incorporates carbon into the growing film. If the insertion reaction (8) has a larger activation energy than the elimination reaction (7), it would explain the observed increase in carbon content with increasing temperature for films deposited in the absence of ammonia (Fig. 7). Both processes leave the titanium centers vulnerable to trace oxygen, raising the impurity content of deposited films.

In the presence of ammonia, the transamination reaction (9) successfully removes the carbon from the deposited film.[11–13]

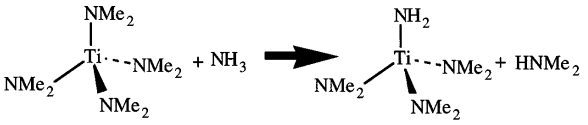

(9)

As mentioned in Sec. IV. B, a ratio of 0.015 NH_3/TDMAT was sufficient to notice the reduction in carbon concentrations,[26] and a ratio of 7 : 1 saturates the reduction. Oxygen levels dropped by half, partially because of the increased growth rate. The carbon content dropped by 80% in some cases. Hydrogen contents fell by 33–50%.

Infrared spectroscopy and mass spectroscopy have found dimethylamine ($HNMe_2$) by-products when TDMAT and NH_3 are mixed, suggesting the transamination reaction (9). Support for this mechanism was found when $HNMe_2$ suppressed TDMAT decomposition (i.e., equilibrium shifted left).[30] Conclusive evidence was provided when isotopic analysis using ND_3 and $^{15}NH_3$ yielded $Ti^{15}N$ and $DNMe_2$.[31,32] Weiller and Partido[33] reported the fast bimolecular rate constant of $(1.1 \pm 0.1) \times 10^{-16}$ cm^3 $molecule^{-1}$ s^{-1} for this reaction.

Four successive transamination reactions [Eq. (9)] would result in the unknown compound titanium tetraamide, $Ti(NH_2)_4$. This compound would be expected to decompose rapidly at high temperatures, by loss of two ammonia molecules, to form titanium diimide, HN = Ti = NH. This unsaturated species would be expected to stick with high probability to the surface of the growing film, thus leading to the low step coverage observed in the presence of ammonia (see Sec. IV. F. 1 below). Thermal removal of some of the nitrogen and hydrogen from the surface of the film would finally result in the observed film stoichiometry.

Greater ammonia concentrations allowed more transamination to occur. The stronger imido bonds resulting from increased transamination may yield denser films and lower resistivities. Denser films have fewer pores and would allow less penetration of the film

by oxygen. This would explain the relatively stable sheet resistance of films deposited with high ammonia concentrations described in Sec. III. E, and at least in part, the drop in resistivity with increasing ammonia concentration.[26,34,35]

F. Applicability

1. Step coverage

Film must be deposited uniformly or the protective ability of the material cannot be applied. Films were deposited on patterned wafers for conformality studies. High-temperature TiN depositions have yielded films with poor step coverage. One might expect that lower temperatures might improve step coverage. A film deposited at 190 °C exhibited poor step coverage (10–30%) when a high concentration of ammonia was used. Lower ammonia concentrations did lead to improved step coverage, although the extreme thinness of the layers made quantification difficult.

2. Diffusion barrier properties

Films using APCVD of TDMAT and NH_3 have been tested elsewhere for suitability as a diffusion barrier[6] and were found to protect an underlying *c*-Si wafer from a gold overlayer at 550 °C. Oxygen, although it increases resistivity, may play a beneficial role in barrier stability. Several studies indicated that TiN films exposed to air provide improved barrier performance relative to unoxidized films.

Use of TiN as a diffusion barrier in microelectronic applications will ultimately depend on the barrier versus conductive properties (i.e., stability and conformality versus resistivity) required under the appropriate circumstances.

V. CONCLUSIONS

TiN thin films have been grown using $Ti(NMe_2)_4$ both with and without NH_3 in an APCVD system. Ammonia was necessary to deposit near stoichiometric TiN ($N/Ti = 1.05 \pm 0.15$) with growth rates of 200–350 Å/min. Both stoichiometry (except for hydrogen) and growth rate were relatively insensitive to temperature as well as to ammonia/TDMAT concentration ratios above 1. The robustness of the process is favorable for manufacturing. H/Ti and film resistivity decrease with an increase in temperature or ammonia concentration. The lowest resistivities were found for films deposited at temperatures between about 300 and 400 °C.

Films grown without ammonia are nitrogen-poor and contain carbon, hydrogen, and oxygen. Much of the oxygen may be from oxidation because of the porous nature of these films. These films were highly resistive, possibly because of the low growth rates and extreme thinness of the TiN layer. Protection from atmospheric contamination may be provided by immediately depositing the appropriate metallization layer.

Films deposited with high ammonia concentrations had high conductivity but poor step coverage. Films deposited with little or no ammonia had improved step coverage but lower conductivity. Ultimately, the use of CVD TiN in microelectronics will depend on an appropriate trade-off between conductivity and step coverage for any particular application.

We have also studied the reaction of tetrakis(diethylamido)titanium, $Ti(NEt_2)_4$, and found that its properties are even more suitable for use in microelectronics.[36]

ACKNOWLEDGMENTS

This work was sponsored by SEMATECH Contract 94062388A-XFR and was conducted in part at the Harvard University Materials Research Laboratory. The authors would like to thank Schumacher for the TDMAT, Watkins-Johnson for the belt furnace, John Thornton for assistance with the chemicals, Anthony Toprac for step coverage data, Pat Slane for the Harwell RBS standard, as well as Glen Wilk, Steve Theis, Frans Spaepen, John Chervinsky, Yuan Lu, Robert Graham, and Seth Kosowsky for assistance in conducting and evaluating RBS, XPS, and XRD spectra. The authors also thank Ellen Sarot for editorial suggestions.

REFERENCES

1. S. R. Kurtz and R. G. Gordon, Thin Solid Films **140**, 277 (1986).
2. W. Tsai, J. Fair, and D. Hodul, in *Advanced Metallization and Processing for Semiconductor Devices and Circuits II,* edited by A. Katz, S. P. Murarka, Y. I. Nissim, and J. M. E. Harper (Mater. Res. Soc. Symp. Proc. **260**, Pittsburgh, PA, 1993), p. 793.
3. Y. Inoue, S. Tanimoto, K. Tsujimura, T. Yamashita, Y. Ibara, Y. Yamashita, and K. Yoneda, J. Electrochem. Soc. **141** (4), 1056 (1994).
4. W. Tsai, M. Delfino, J. A. Fair, and D. Hodul, J. Appl. Phys. **73** (9), 4462 (1993).
5. M. Mandl, H. Hoffman, and P. Kucher, J. Appl. Phys. **68** (5), 2127 (1990).
6. J. N. Musher and R. G. Gordon, J. Electronic Mater. **20**, 1105 (1991).
7. I. J. Raaijmakers, R. N. Vrtis, J. Yang, S. Ramaswami, A. Lagendijk, D. A. Roberts, and E. K. Broadbent, in *Advanced Metallization and Processing for Semiconductor Devices and Circuits II,* edited by A. Katz, S. P. Murarka, Y. I. Nissim, and J. M. E. Harper (Mater. Res. Soc. Symp. Proc. **260**, Pittsburgh, PA, 1993), p. 99.
8. S. Chiang, R. Hendel, and F. Zhang, in *Advanced Metallization and Processing for Semiconductor Devices and Circuits II,* edited by A. Katz, S. P. Murarka, Y. I. Nissim, and J. M. E. Harper (Mater. Res. Soc. Symp. Proc. **260**, Pittsburgh, PA, 1993), p. 813.
9. J. B. Price, J. O. Borland, and S. Selbrede, Thin Solid Films **236**, 311 (1993).
10. D. C. Bradley and I. M. Thomas, J. Chem. Soc., 3857 (1960).
11. R. M. Fix, R. G. Gordon, and D. M. Hoffman, Chem. Mater. **2**, 235 (1990).

12. R. M. Fix, R. G. Gordon, and D. M. Hoffman, Chem. Mater. **3**, 1138 (1991).
13. R. M. Fix, R. G. Gordon, and D. M. Hoffman, in *Chemical Vapor Deposition of Refractory Metals and Ceramics*, edited by T. M. Besmann and B. M. Gallois (Mater. Res. Soc. Symp. Proc. **168**, Pittsburgh, PA, 1990), p. 357.
14. D. Roberts, Schumacher Corporation, private communication.
15. J. L'ecuyer, J. A. Davies, and N. Matsunami, Nucl. Instrum. Methods **160**, 337 (1979).
16. C. Cohen, J. A. Davies, A. V. Drigo, and T. E. Jackman, Nucl. Instrum. Methods in Phys. Res. **218**, 147 (1983).
17. W-K. Chu, J. W. Mayer, and M. A. Micolet, *Backscattering Spectrometry* (Academic Press, Orlando, FL, 1978).
18. L. C. Feldman and J. W. Meyer, *Fundamentals of Surface and Thin Film Analysis* (Elsevier Science Publishers, Amsterdam, 1986).
19. A. Turos and O. Meyer, Nucl. Instrum. Methods in Phys. Res. **B4**, 92 (1984).
20. T. C. Huang, R. Gilles, and G. Will, Thin Solid Films **230**, 99 (1993).
21. L. M. Goldman and D. T. Wu, private communication.
22. I. J. Raaijmakers *et al.*, Thin Solid Films **247**, 85 (1994).
23. I. J. Raaijmakers, R. N. Vrtis, G. S. Sandhu, J. Yang, E. K. Broadbent, D. A. Roberts, and A. Lagendijk, *Proc. 9th Int. IEEE VLSI Multilevel Interconnection Conference* (IEEE, New York, 1992).
24. I. J. Raaijmakers, J. Yang, M. G. Fissel, and K. B. Levy, *SEMI Technology Symposium* (Semicon, Japan, December, 1992).
25. R. Chowdhury, X. Chen, and J. Narayan, Appl. Phys. Lett. **64** (10), 1236 (1994).
26. A. Katz, A. Feingold, S. Nakahara, S. J. Pearton, E. Lane, M. Geva, F. A. Stevie, and K. Jones, J. Appl. Phys. **71** (2), 993 (1992).
27. A. Weber, R. Nikulski, C-P. Klages, M. E. Gross, W. L. Brown, E. Dons, and R. M. Charatan, J. Electrochem. Soc. **141** (3), 849 (1994).
28. G. A. Dicit, C. C. Wei, F. T. Liou, and H. Zhang, Appl. Phys. Lett. **62**, 357 (1993).
29. Z. Pang, M. Boumerzoug, R. V. Kruzelecky, P. Mascher, J. G. Simmons, and D. A. Thompson, J. Vac. Sci. Technol. A **12** (1), 83 (1994).
30. L. H. Dubois, B. R. Zergarski, and G. Girolami, J. Electrochem. Soc. **139** (12), 3603 (1992).
31. J. A. Prybyla, C-M. Chiang, and L. Dubois, J. Electrochem. Soc. **140** (9), 2695 (1993).
32. J. A. Prybyla, C-M. Chiang, and L. Dubois, in *Chemical Perspectives of Microelectronic Materials III*, edited by C. R. Abernathy, C. W. Bates, D. A. Bohling, and W. S. Hobson (Mater. Res. Soc. Symp. Proc. **282**, Pittsburgh, PA, 1993), p. 287.
33. B. H. Weiller and B. V. Partido, Chem. Mat. **6** (3), 260 (1994).
34. S. C. Sun and M. H. Tsai, Thin Solid Films **253**, 440 (1994).
35. G. Sandhu, S. G. Meikle, and T. T. Doan, Appl. Phys. Lett. **62** (3), 240 (1993).
36. J. N. Musher and R. G. Gordon, J. Electrochem. Soc. **143**, 736 (1996).